Evolution of black silicon nano- and micro-scale surface topologies upon femtosecond laser irradiation

S. I. Kudryashov,[a] E. V. Golosov,[b] A. A. Ionin,[a] Yu. R. Kolobov,[b] A. E. Ligachev,[c]
S.V. Makarov,[a] Yu. N. Novoselov,[a] L. V. Seleznev,[a] D. V. Sinitsyn,[a]
[a] P.N. Lebedev Physics Institute, Moscow, Russia
[b] Belgorod State University, Belgorod, Russia
[c] A.M. Prokhorov General Physics Institute, Moscow, Russia

ABSTRACT

Gradual evolution of silicon surface topology from one-dimensional to two-dimensional nanogratings and then to isotropic sets of nanospikes was observed by increasing IR and UV femtosecond laser irradiation dose (the variable number of incident laser pulses at the constant laser fluence). The fundamental mechanisms of these topological transformations are discussed.

Keywords: femtosecond laser pulses, "black" silicon, surface nano- and microstructuring

I. INTRODUCTION

Femtosecond (fs) laser nano- and microstructuring of silicon surfaces appears as a promising way in fabricating highly-sensitive silicon substrates for surface-enhanced Raman scattering (SERS)[1] and strongly-absorbing silicon photodetectors,[2] with their unique optical characteristics provided by isotropic arrays of nano-spikes and micro-columns, respectively.[1,2] Although technological perspectives of these fs laser surface modification techniques in fabricating such nano- and microstructured silicon devices are quite distinct, clear understanding of fundamental physical mechanisms involving effects of laser polarization (vector $\boldsymbol{e}$), wavelength λ and pulse duration, laser fluence F, and the number of incident pulses N on topologies and other physical or chemical characteristics of the resulting surface structures.
In this work, we studied the effect of fs laser irradiation time (the number of incident pulses N) on topologies of silicon surface nanostructures fabricated by IR (744 nm) and UV (248 nm) fs laser pulses, in terms of microscopic physical mechanisms of nano- and micro-scale surface modification.

II. EXPERIMENTAL SETUP AND SAMPLES

The experiments were performed on an experimental setup including a Ti:sapphire laser (Avesta Project) with fundamental radiation pulses (central wavelength is 744 nm, the FWHM of the lasing band is about 15 nm) with a duration of about 80 fs (FWHM) and an energy of up to 8 mJ.[3] The transverse spatial distribution of the laser field corresponded to the TEM00 mode. Normally, incident laser radiation was focused on a spot with a diameter of 1.2 mm (at a level of $1/e^2$) on the surface of a target [commercial undoped silicon Si(100) wafers]. The target was placed onto a computer-controlled three-dimensional motorized stage (Fig.1). The energy of laser pulses was varied and controlled by, respectively, a reflecting polarization attenuator (Avesta Project), pyroelectric energymeter (OPHIR) and a DET-210 calibrated photodiode (Thorlab) illuminated by a weak laser beam split through a steering dielectric mirror. The writing of nanostructures was performed by irradiating different spots of the stationary silicon target surface by the different number of laser pulses N = 100, 300 and 1000 at low IR fs-laser radiation energies (< 0.5 mJ, peak power W < 4 GW) in order to avoid a noticeable degradation of the energy density distribution on the target surface associated with self-focusing in air (the critical self-focusing power is $W_{cr} \approx 3$GW[4]) and the accompanying effects of chromatic emission, filamentation, and scattering on a plasma.[4,5] Topological characterization of fs laser-fabricated nano- and micro-scale

surface structures was performed by means of a scanning electronic microscope (SEM) Quanta FEG at magnification up to 100 000×.

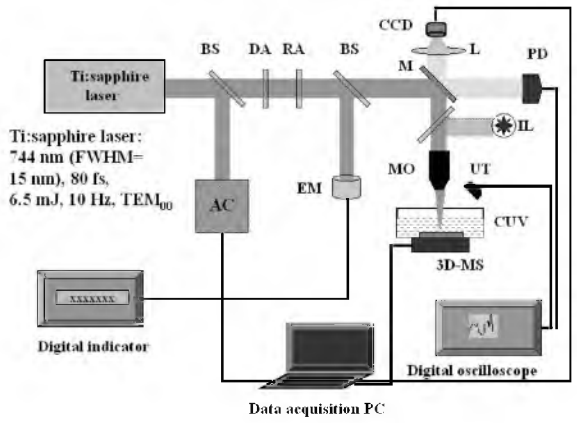

Figure 1. Experimental setup for femtosecond laser surface nanostructuring of solids: BS – beam splitter, AC – autocorrelator for laser pulsewidth measurements, DA, RA – variable diffractive and reflective energy attenuators, EM – thermocouple energy meter, M – mirror, L – focusing fused silica lens, CCD – charge-coupled device camera for surface imaging, PD – fast trigger silicon photodiode, IL – illumination lamp, MO – micro-objective, UT – ultrasonic transducer, CUV – glass cuvette with the silicon sample, 3D-MS – three-dimensional motorized micro-stage.

III. EXPERIMENTAL RESULTS AND DISCUSSION

The UV fs-laser nanostructured silicon surface spots demonstrated at $F \approx 0.08$ J/cm^2 and $N \approx 100$ pulses well-defined one-dimensional nanogratings (Fig.2) with periods $\Lambda \approx 0.5$-0.6 μm oriented perpendicularly to the polarization of the laser electric field $\boldsymbol{E}$ (grating wavevector $\boldsymbol{q} \parallel \boldsymbol{v},\boldsymbol{E}$) and a simple two-dimensional Fourier spectrum of the nanostructures indicating their regular one-dimensional character (see the lateral reflexes in Fig.3). At higher laser irradiation doses ($F \approx 0.08$ J/cm^2, $N \approx 300$ pulses) the regular nanogratings have got their lines damaged via their breaking (Fig.4), represented by significant reduction of the lateral reflexes in the Fourier spectrum and the simultaneous rise of the isotropic component amplitude (central bright spot in Fig.5). The close view at the breaking points (Fig.6) showed a number of round-shaped fragments and droplet-like spikes indicating that the instability of the gratings resulted from displacement of molten fragments of the gratings, potentially, via nano-scale capillary effects. Moreover, the transverse nanopores

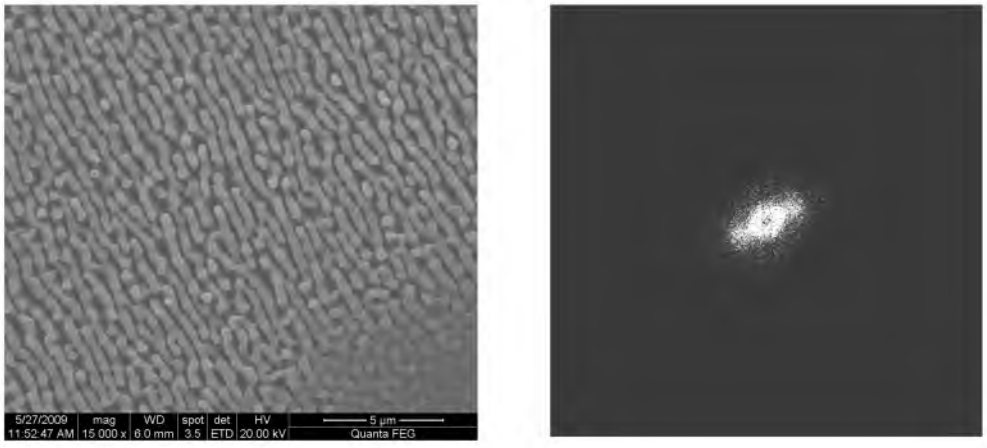

Figure 2 (left). Low-magnification SEM image of Si surface nanostructured in air at $F \approx 0.08$ J/cm^2 and $N \approx 100$ pulses.
Figure 3 (right). Fourier spectrum of the surface nanostructure given in Fig.2.

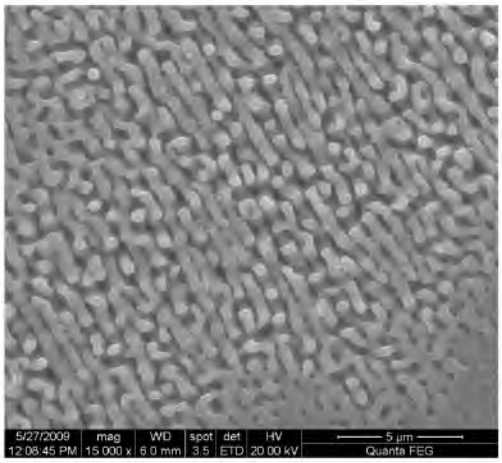

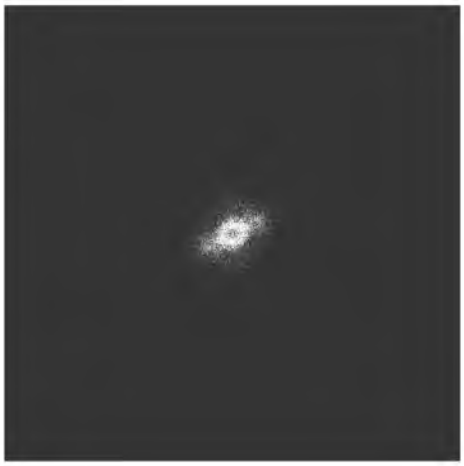

Figure 4 (left). Low-magnification SEM image of Si surface nanostructured in air at $F \approx 0.08$ J/cm^2 and $N \approx 300$ pulses.
Figure 5 (right). Fourier spectrum of the nanostructure given in Fig.4.

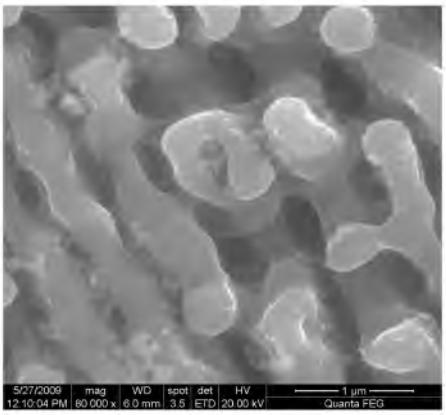

Figure 6. High-magnification SEM image of Si surface nanostructured in air at $F \approx 0.08$ J/cm^2 and $N \approx 300$ pulses.

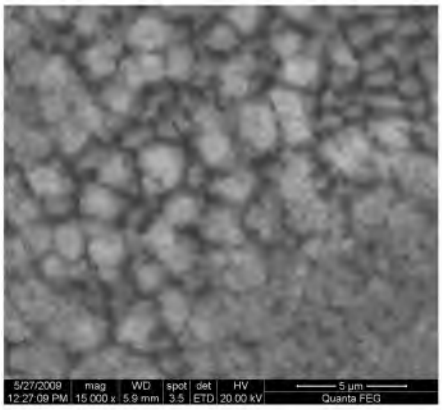

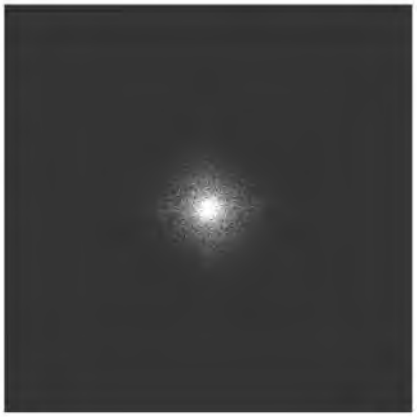

Figure 7 (left). Low-magnification SEM image of Si surface nanostructured in air at $F \approx 0.08$ J/cm^2 and $N \approx 1\times10^3$ pulses.
Figure 8 (right). Fourier spectrum of the surface nanostructure given in Fig.7.

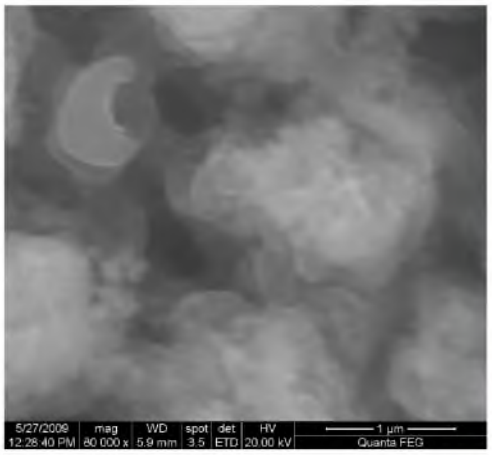

Figure 9 (left). High-magnification SEM image of Si surface nanostructured in air at $F \approx 0.08$ J/cm^2 and $N \approx 1\times10^3$ pulses.
Fig.10 (right). Real-scale optical image of a highly-absorbing fs-laser nanostructured "black" region on a silicon wafer.

between the nanospikes clearly visible in Fig.6 on its right side, but not very pronounced in the larger-scale Fourier spectrum in Fig.5, demonstrated approximately a double period ≈ 1 μm. Finally, at the maximum laser irradiation dose ($F \approx 0.08$ J/cm^2, $N \approx 10^3$ pulses) the grating-like structure completely disappeared in the surface topology (Fig.7), resulting via the abovementioned breakage process in an isotropic set of nanospikes, as shown in the corresponding Fourier spectrum in Fig.8. These nanospikes exhibited a significant amount of amorphous silicon flakes resided on them via the ongoing vaporization and re-deposition processes (Fig.9). Therefore, the observed transformations of the silicon surface nanotopology occur at higher and higher surface temperatures, consequently involving melting ($T_{melt} = 1.6\times10^3$ K)[6] and vaporization ($T_{boil} = 2.5\times10^3$ K)[6] processes versus increasing laser irradiation dose. This fact appears to reflect the gradually rising absorbance of the nanostructured silicon surface, finally resulting in the strongly-absorbing "black" silicon[7] (Fig.10).

Likewise, the IR fs-laser nanostructured silicon surface spots demonstrated at $F \approx 0.023$ J/cm^2 and $N \approx 100$ or 300 pulses well-defined or considerably degraded one-dimensional gratings oriented perpendicularly to the polarization of the laser (left and central images in Figs.11,12), respectively, while at higher $N \approx 10^3$ pulses the gratings were almost completely corrupted revealing presumably isotropic micro-columns (right images in Figs.11,12). Again, at higher N we observed clear indications of melting of the grating lines and following bonding between neuboughring ones, finally resulting in rather isotropic sets of micro-spikes covered by amorphous residue (Fig.13). The observed similarity between these IR and UV studies indicated the rather universal character of such nanoscale surface topology evolution, going through a highly ordered one-dimensional structure to partially and completely disordered ones.

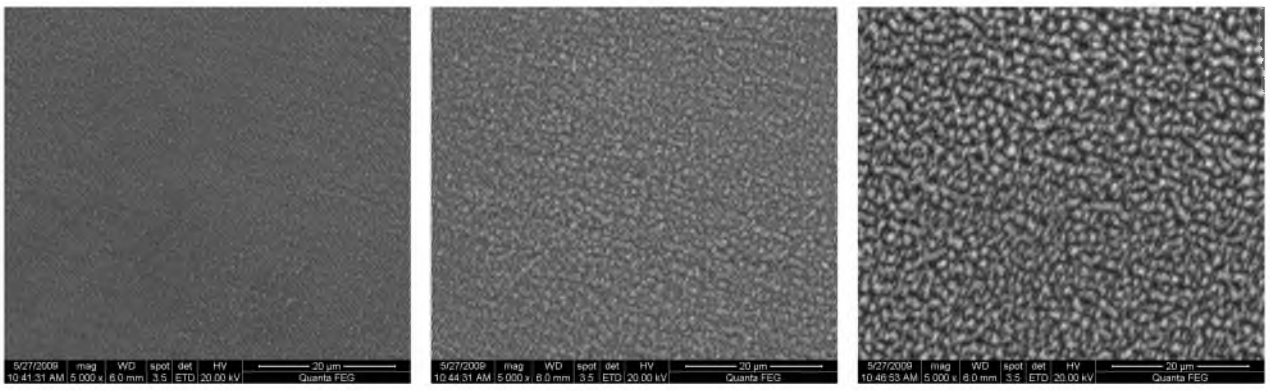

Figure 11. Low-magnification SEM image of Si surface nanostructured in air at $F \approx 0.023$ J/cm^2 and $N \approx 100$ (left), 300 (center) and 1×10^3 pulses (right).

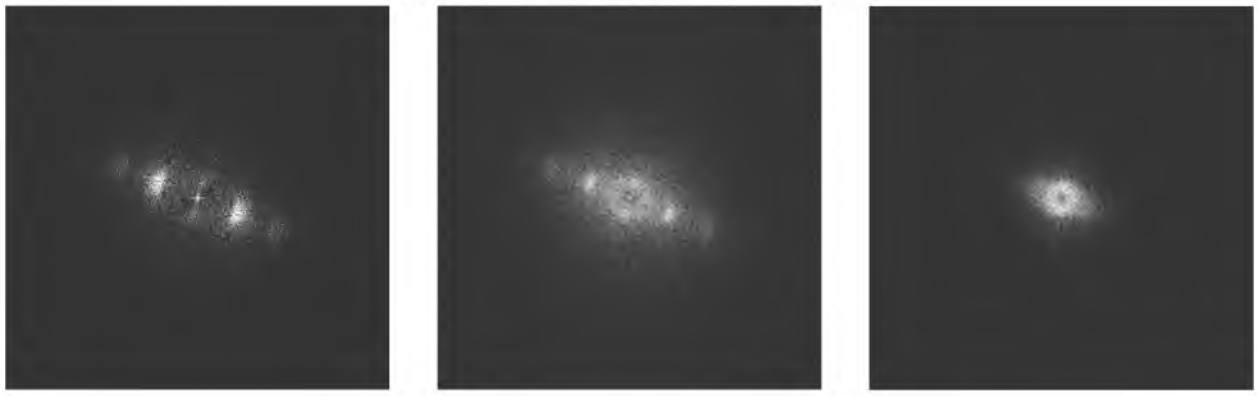

Figure 12. Fourier spectra corresponding to the SEM surface images in Fig.11.

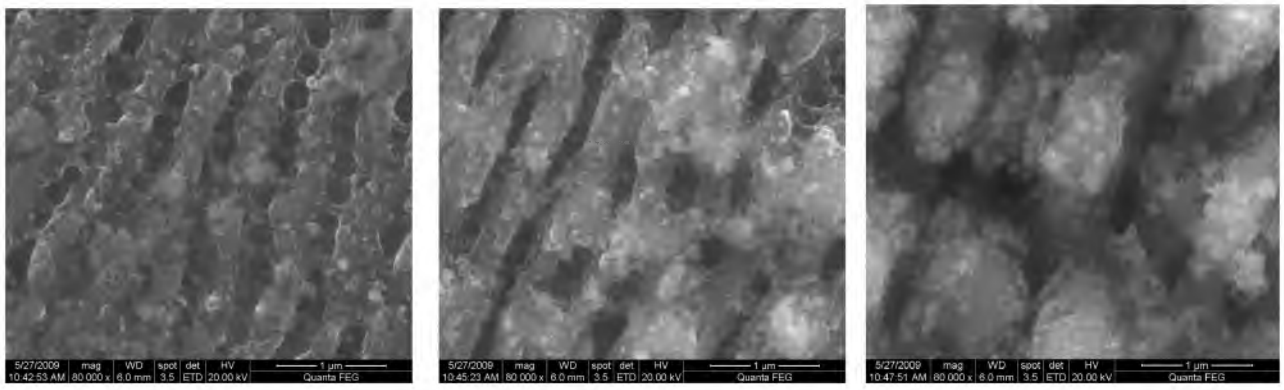

Figure 13 (left). High-magnification SEM images of Si surface nanostructured in air at $F \approx 0.08$ J/cm^2 and $N \approx 100$ (left), 300 (center) and 1×10^3 pulses (right).

IV. CONCLUSIONS

In conclusion, in this study we have experimentally identified basic physical steps underlying destructive evolution of IR and UV femtosecond laser fabricated nanostructures on silicon wafer surfaces starting from regular one-dimensional nanogratings, finally, to isotropic sets of micro-columns.

REFERENCES

1. E.D. Diebold, P. Peng, and E. Mazur, J. Am. Chem. Soc. **131**, 16356, 2009; E.D. Diebold, N.H. Mack, S.K. Doorn, and E. Mazur, Langmuir **25**, 1790, 2009.
2. Z. Huang, J.E. Carey, M. Liu, X. Guo, E. Mazur, and J.C. Campbell, Appl. Phys. Lett. **89**, 033506, 2006; R.A. Myers, R. Farrell, A. Karger, J.E. Carey, and E. Mazur, Appl. Opt. **45**, 8825, 2006.
3. E. V. Golosov, V. I. Emel'yanov, A. A. Ionin, Yu. R. Kolobov, S. I. Kudryashov, A. E. Ligachev, Yu. N. Novoselov, L. V. Seleznev, and D. V. Sinitsyn, JETP Letters **90**, 107, 2009.
4. A. Couairon and A. Mysyrowicz, Phys. Rep. **441**, 47, 2007.
5. S. M. Klimentov, T. V. Kononenko, P. A. Pivovarov, et al., Quantum Electron. **32**, 433, 2002.
6. I.S. Grigor'ev, E.Z. Meylikhov (ed.), *Fizicheskie velichini*, Energoatomizdat, Moscow, 1991.
7. B.R. Tull, J.E. Carey, E. Mazur, J. McDonald, and S.M. Jalisove, Mat. Res. Soc. Bull. **31**, 626, 2006.